



Influence of Urban Land Use Land Cover Changes on Land Surface Temperature in Dar es Salaam Metropolitan City, Tanzania: The Use of Geospatial Approach

Olipa Simon^{1*}, Nestory Yamungu² and James Lyimo¹

¹*Institute of Resources Assessment, University of Dar es Salaam, P. O. Box 35097, Dar es Salaam, Tanzania.*

²*Department of Geography, University of Dar es Salaam, P. O. Box 35049, Dar es Salaam Tanzania.*

*Corresponding author's e-mail address: olipasimon@gmail.com

Received 31 Aug 2022, Revised 10 May 2023, Accepted 22 May 2023 Published June 2023

DOI: <https://dx.doi.org/10.4314/tjs.v49i2.7>

Abstract

Land use land cover (LULC) changes affect the planet's energy balance and region's climate. Land Surface Temperature (LST) is a vital indicator of this change. Studies in Dar es Salaam Metropolitan City have investigated LST and its relationships with building heights and densities, urban heat islands, spectral indices, and urban morphological determinants. The present study used cross-sectional profiles, chord diagrams, and simple linear regression models to examine the influence of LULC changes on the LST in Dar es Salaam Metropolitan City (DMC). LST was extracted from Landsat 5 TM and 8 OLI/TIRS images for 1995, 2009, and 2017. LULC was identified via the supervised random forest classification algorithm. Between 1995 and 2017, built-up areas rose by 8%, vegetation fell 7%, and bare soil 3%. As a result, the average LST rose by 3 °C. Built-up areas had the highest temperatures (24–26.5 °C), followed by bare soil (22–25.5 °C). The lowest temperatures (21–25 °C) were on vegetation and water. Built-up area positively correlated with LST, while vegetation, water bodies, and bare soil negatively correlated. The study results can assist local authorities in enforcing urban planning regulations, raising public awareness, and guiding policymakers in creating sustainable planning and management strategies for the future.

Keywords: Dar es Salaam, Land use land cover, simple linear regression model, land surface temperature, chord diagrams.

Introduction

Rapid urbanisation poses threats to the world, with more than half (about 57%) of the global population currently living in urban areas and an expected increase to approximately 68% by 2050, where Sub-Saharan African countries are anticipated to have more than half the world's population by 2050 (United Nations 2019b, Demographia 2022). Additionally, it is projected that approximately half of the global population growth by 2050 will be concentrated in nine specific countries: India, Nigeria, Pakistan,

Democratic Republic of Congo, Ethiopia, United Republic of Tanzania, United States of America, Uganda and Indonesia (United Nations 2019a). Due to rising urbanisation, people want additional land for housing and infrastructure. In addition, they need extra fuel, industrial minerals, and building materials. Consequently, impervious surfaces raise the land surface temperature (LST), significantly hurting people's livelihood as excess heat is stored and accelerates to high temperatures (Simwanda et al. 2019). Furthermore, the change in the land surface

environment through activities such as construction and landscaping has had detrimental impacts on the environment's energy balance, boosting sensible heat instead of latent heat and making it hotter than it would be under natural conditions, where the energy balance remains undisturbed by these human activities (Ibrahim et al. 2016). Increased LST generates hot days and warm spells, worsening cities' urban heat island (UHI) impacts (Zhang and Sun 2019). UHI refers to the phenomenon in which urban areas experience higher temperatures than the surrounding rural or undeveloped areas (Sussman et al. 2019). Urban regions use artificial materials, mainly concrete and asphalt, for building, which contribute to temperature disparities, affect urban environment islands, and has local and global impacts (Mensah et al. 2020). UHI affects people's lives. High temperatures, especially in dry season, increase demands for air conditioning to cool buildings, increase energy consumption, increase air pollutants, impair thermal comfort, and harm the environment.

Urbanisation has been rapidly transforming Tanzania's land use land cover, particularly in the city of Dar es Salaam (Mnyali and Materu 2021). Dar es Salaam is the fastest-growing city in Tanzania, with a population of 5.4 million residents, aiming to exceed 13 million by 2035 and 16 million by 2040 and expected to become the fourth most populous city in Africa, with Luanda and Johannesburg being close behind (Bello-Schünemann and Aucoin 2016, United Republic of Tanzania 2022). It is anticipated that, soon, it will rank as the fourth most populous city. Therefore, it is crucial to research the implications of land use land cover changes and their impacts on land surface temperature to make informed decisions for the city's future development.

Extensive research has been conducted on the relationships between Land use Land cover (LULC) and Land Surface Temperature (LST) in various parts of the world. For instance, studies in Paço do Lumiar, Brazil (Serra et al. 2018), Botswana (Akinyemi et

al. 2019), and Pune City, India (Gohain et al., 2020) have investigated the effects of LULC changes on LST trends. In Gaborone, Botswana (Akinyemi et al. 2019) specifically examined the impact of LULC changes on land surface temperature trends in an urbanising dryland region of Africa. Gohain et al. (2020) focused on Pune City, India, to assess the influence of LULC changes on land surface temperature. Similarly, researchers in Jordan and Raipur City, India, namely Jaber (2019) and Guha et al. (2020), respectively, utilised remote sensing (RS) data to explore how LULC changes affect LST. They employed remote sensing techniques to understand the relationships between LULC and surface temperature. Xiao et al. (2018) analysed both Vienna and Madrid, investigating the responses of LST to LULC changes. Their study utilised regression models to comprehend the interactions between these two cities' LULC and LST. Additionally, Naim and Kafy (2021) conducted research in Chattogram City, Bangladesh, using regression models to explore the relationships between LST and LULC.

Geographic Information Systems (GIS) and Remote Sensing (RS) are effective and affordable tools for analysing LULC changes. Remote sensing data are widely used for detecting, measuring, and mapping LULC patterns due to their frequent data collection, processing suitability, and precise georeferencing (Tewabe and Fentahun 2020). In Dar es Salaam, GIS and RS were utilised to determine LULC (Kibassa and Shemdoe 2016, Mzava et al. 2019, Manyama et al. 2020). However, limited studies have examined the influence of LULC on LST using GIS and RS. Although these researchers examined the association between LULC and LST using geospatial technology in diverse places worldwide, there needs to be more understanding of urban LULC on LST and urban heat islands, notably in Tanzania. LULC with LST correlation helps comprehend the earth's biophysical makeup, analyse ramifications, and provide solutions to mitigate impacts for effective urban planning and management. This study

assessed the impacts of urban LULC alterations on urban LST in Dar es Salaam Metropolitan City (DMC). The study intended to answer the following questions: i) How has LULC changed over the past two decades? ii) What are the spatial patterns of LST?; iii) Which LULC has more significant effects on LST?; and iv) How does LULC correlate with LST? The findings help inform decision-makers, land managers and planners, and architects about managing natural resources sustainably and mitigating the effects of LST caused by the rapidly growing metropolitan cities such as Dar es Salaam.

Materials and Methods

Description of the study area

The study was conducted in Dar es Salaam Metropolitan City (DMC), located between the latitudes of 6.36° and 7.0° South of the equator and the longitudes of 39.0° and 33.33° East of Greenwich (Figure 1). The city has five districts (Kinondoni, Ubungo, Ilala, Temeke and Kigamboni), covering a total area of 1,393 km². Due to its proximity to the equator and the warm Indian Ocean, the city is one of Tanzania's warmest regions, with annual mean maximum and minimum temperatures ranging from 29 to 32 °C (December–March) and 19 to 25 °C (June–September), respectively (Simon et al. 2022). In addition, DMC is Tanzania's financial and port hub, "commercial capital", and a national hub for industry, education, and culture, creating huge job prospects and attracting rural immigration.

Data collection

Data types and sources

This study used Landsat images acquired from the USGS website (<https://earthexplorer.usgs.gov>). The area is clouded almost throughout the year; as a result, obtaining clear sky images at regular intervals and the same month was challenging (cloud cover less than 10%). Therefore, the satellite imageries selected were for 1995, 2009 and 2017, falling within the same season (June to July) data acquisition window (Table 1). Two were images from the Landsat 5 TM sensor (1995 and 2009), while the third was Landsat 8 (2017). Landsat TM consists of seven spectral bands with a spatial resolution of 30 metres for optical bands (Bands 1 to 5 and 7) and a thermal infrared band (Band 6) with a spatial resolution of 120 metres. While Landsat 8 consists of eleven bands from Operational Land Imager (OLI) and Thermal Infrared Sensor (TIRS). Whereby nine OLI spectral bands with a spatial resolution of 30 metres for Bands 1 to 7 and Thermal Infrared Sensor (TIRS) Bands 10 and 11 (100 m resolution). The optical bands were used to classify the land use land cover in the study area, while the thermal infrared bands were used to generate land surface temperatures. However, for Landsat OLI, TIR band 10 was chosen as a single spectral band rather than a split window algorithm due to the more significant calibration uncertainty associated with TIR band 11 (Guha et al. 2018).

Table 1: Attributes of satellite imageries used

Sensor	Path	Row	Date of acquisition
Landsat 5 (TM)	166	65	25 June 1995
Landsat 5 (TM)	166	65	01 July 2009
Landsat 8 (OLI)	166	65	25 June 2017

Image processing and classification

Before image classification, Landsat images were preprocessed (atmospheric and radiometric correction, cloud filling, and masking) in Google Earth Engine's code editor to remove the sensor, atmospheric, and illumination artefacts (Young et al. 2017).

Then, using R's Random Forest Classifier, supervised classification was performed. Random Forest (RF) is the most used machine-learning remote sensing (RS) land use land cover classification. RF is popular because it can handle outliers and noisy datasets; its accuracy with multi-source high-

dimensional datasets is higher than other popular classifiers (Noi Phan et al. 2020). Due to the limited spatial resolution of the images, we used higher resolution images from Planet, Bing Maps, Esri, and Google Earth using QGIS plugins to generate accurate training signatures for each LULC. Finally, the images were classified into four LULC categories: water (rivers, ponds, wetlands, and ocean), bare soil (sand, exposed soil, and un-vegetated areas), vegetation (forestlands, bushlands, agricultural lands, and other vegetative surfaces) and built-up (buildings, roads, and other impervious surfaces). Next, accuracy assessments were performed to assess the accuracy of the LULC classification. First, 123 ground-truthing points were collected using historical Google Earth high-resolution images. Then, the confusion matrix and kappa coefficients were calculated to determine the accuracy of the classified images. The overall accuracy of the images varied between 90% and 94.55%, while the

kappa coefficient varied between 0.902 and 0.819, indicating excellent accuracy in classified images. Erdas Imagine 2014 software was used to conduct the accuracy assessments.

Retrieval of land surface temperature

Landsat imageries' thermal band(s) were used to calculate the land surface temperature (LST). Band 6 (10.40–12.50 m) is the Landsat 5 (TM) thermal band. Band 10 (10.6–11.19 m) and Band 11 (11.5–12.51 m) are the thermal bands on the Landsat 8 (OLI). The LST is obtained in two steps. The thermal band's Digital Number (DN) was first converted to spectral radiance. The second step was to convert the spectral value of radiance to degrees Celsius at-satellite brightness temperature. For Landsat 5 TM and Landsat 8 (OLI), the DN to radiance conversion was performed using equation (1) and equation (2), which are supplied in the corresponding sensor's handbook.

$$L_{\lambda} = \left(\frac{L_{max\lambda} - L_{min\lambda}}{QCal_{max} - QCal_{min}} \right) * (QCal - QCal_{min}) + L_{min\lambda} \tag{1}$$

Where; L_{λ} = sensor radiance, $L_{max\lambda}$ = maximum radiance of thermal band, $L_{min\lambda}$ = minimum radiance of thermal band, $QCal$ = quantised calibrated pixel value in DN, $QCal_{max}$ = maximum quantised calibrated pixel value in DN (DN=255), $QCal_{min}$ = minimum quantised calibrated pixel value in DN (DN=0).

$$L_{\lambda} = (M_L * QCal) + A_L \tag{2}$$

Where; M_L = radiance multiplicative scaling factor, A_L = radiance additive scaling factor for band (obtained from band 10 and 11 metadata file), and $QCal$ = pixel value in DN. The second step was to change the spectral value of radiance to at-sensor brightness temperature (BT ; °Celsius) after converting DN to spectral radiance equation (3).

$$BT = \frac{K_2}{\ln\left(\frac{K_1}{L_{\lambda}} + 1\right)} - 273.15 \tag{3}$$

where K_1 and K_2 are the calibration constants of thermal bands. However, the earth is not a black body and has different underlying surface conditions in different

places. Land surface temperature (T_s), different from at-satellite brightness temperature (BT), is then calculated using equation (4).

$$T_s = \frac{BT}{\left\{1 + \left[\frac{\lambda BT}{p}\right] \ln \epsilon_{\lambda}\right\}} \tag{4}$$

Where; T_s is the LST in °Celsius, BT is the at-sensor BT (°Celsius), λ ($\approx 11.5 \mu m$) is the effective wavelength of emitted radiance,

$$p = h\left(\frac{c}{\sigma}\right) = 1.438 \times 10^{-2} \text{ mK} \tag{5}$$

where σ is the Boltzmann constant ($1.38 \times 10^{-23} \text{ J K}^{-1}$), h is Planck's constant ($6.626 \times 10^{-34} \text{ J sec}$), c is the light velocity of light ($2.998 \times 10^8 \text{ m/s}$), and ϵ_{λ} is the emissivity calculated in (Sekertekin and Bonafoni 2020) using equation (6).

$$\epsilon = 0.004 * P_v + 0.986 \tag{6}$$

where; P_v = proportion of vegetation, as calculated via equation 7.

$$P_v = \left(\frac{NDVI - NDVI_{min}}{NDVI_{max} - NDVI_{min}} \right)^2 \tag{7}$$

NDVI is the Normalised Difference Vegetation Index calculated from Landsat images' Red and Near-Infrared bands. The

methodological approach for this study is summarised in Figure 1.

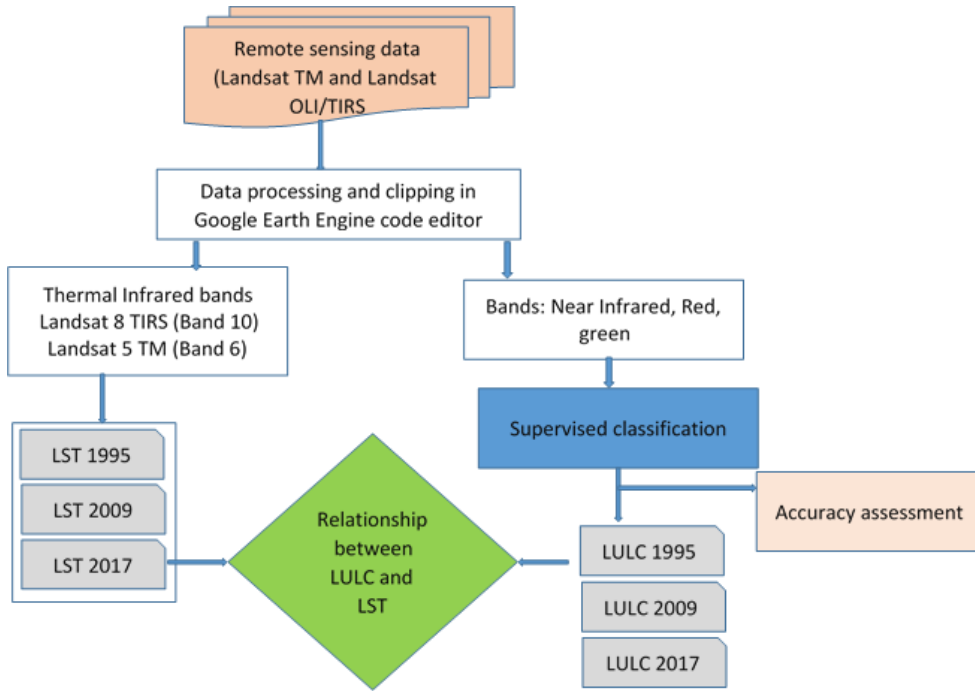


Figure 1: Flowchart of the methodology used in the study.

Defining the relationships between LULC and LST

The relationships between different variables can be determined in a variety of ways. First, a graph or a model can compare the relationships. For example, the mean, minimum, maximum, and standard deviation can create a graphical comparison, while a simple linear regression model (SLRM) can investigate the relationships between variables. The SLRM uses a straight line to measure the connection between two independent variables. According to Iqbal (2021), the main benefit of linear regression over more complex methods like machine learning is its ease of use as an optimisation algorithm, providing strong solutions and allowing for easy and efficient implementation, even on systems with low computational capacity. The mathematical equation of linear regression is easy to understand and has a lower time complexity than other machine

learning algorithms. Linear regression is particularly useful for modelling datasets with linear separability, allowing for identifying and comprehending relationships between variables. Thus, the SLRM and graphical comparison were used to assess the relationships between LULC and LST from 1995 to 2017. The graphical comparison depicts changing mean, minimum, and maximum LST patterns. In addition, from 1995 to 2017, LST profiling was performed to delineate LST change spatially over time in the research area. In this context, the SLRM was used to compute the relationships between each independent variable, i.e., vegetation, built-up area, bare soil and waterbody) against the dependent variable (LST) using the following equation:

$$y = \beta_0 + \beta_1 x + \varepsilon \quad (8)$$

Where; y is the dependent variable, x is the independent variable, and ε is a random error.

Results and Discussion

Land use land cover changes in the city.

From Table 2, the results show that there have been significant changes in land use land cover (LULC) in the study area over time. In 1995, most of the land was covered by vegetation (91%), followed by built-up areas (6%), waterbodies (2%), and bare soil (1%). However, in 2009, there was a noticeable decrease in vegetation coverage by 4%, accompanied by the expansion of built-up areas by 3%. On the other hand, the coverage of waterbodies and bare soil remained relatively stable. The changes in land usage and coverage experienced a more striking shift in 2017 compared to previous years. During this time, vegetation coverage decreased to 84%, while built-up areas

expanded to 13%. Bare soil coverage also reduced to 0%, which may indicate that more of the land is being developed or built. However, waterbody coverage remained stable.

Urbanisation and economic growth may explain the increase in built-up areas at the expense of vegetation and bare soil in the Dar es Salaam Metropolitan City as reported in the previous studies by Mzava et al. (2019) and Mnyali and Materu (2021). The changes in LULC can be visually represented over time through Figure 2, which illustrates that the built-up area starts small and gradually increases, resulting in a redder colouration (since the built-up area is depicted in red).

Table 2: Land use land cover (LULC) percentage in different years

LULC class	1995		2009		2017	
	Sq. km	%	Sq. km	%	Sq. km	%
Waterbody	25	2	28	2	26	2
Vegetation	1,482	91	1,427	87	1,375	84
Bare soil	18	1	22	1	7	0
Built-up	92	6	151	9	217	13

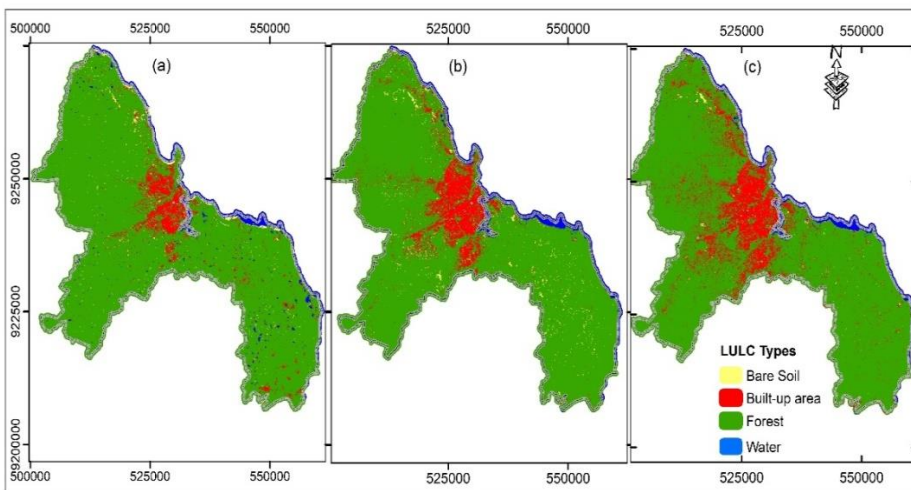


Figure 2: LULC map of Dar es Salaam Metropolitan City in (a) 1995; (b) 2009; and (c) 2017.

Overall temporal and spatial patterns of land surface temperature (LST) of the city

The mean LST in 1995 was 22.37 °C, while in 2009 was 22.43 °C, a 0.06 °C increase from 1995 to 2009. In contrast, mean LST rose by over 2.9 °C between 1995 and

2017, from 22.43 °C to 25.32 °C (Table 3), a 13% rise in the last decade. Similar results have also been found by Kabanda (2019), who investigated the urban heat island analysis in Dar es Salaam, Tanzania.

Table 3: Descriptive statistics of land surface temperature (LST) (°C)

Year	Min	Max	Mean	SD
1995	16.55	27.95	22.37	1.11
2009	16.56	50.29	22.43	1.33
2017	17.25	31.85	25.32	1.34

The LST is coloured grey, blue, and red on maps. The extent of the red region in the 1995 LST map (Figure 3 a) is less than in 2009 (Figure 3 b), showing that the area with

high LST rose in 2009. The area with higher LST also increased considerably in 2017 (Figure 3 c).

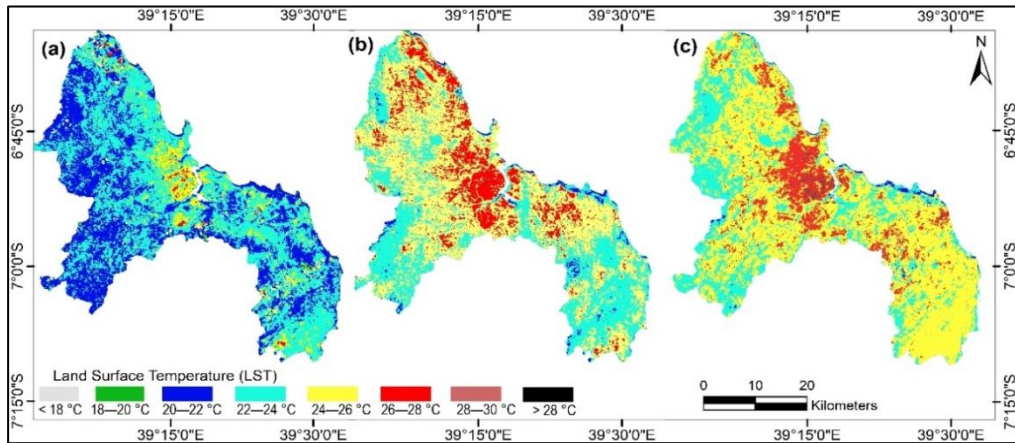


Figure 3: LST map of Dar es Salaam Metropolitan City in (a) 1995; (b) 2009; (c) 2017.

Further analysis by considering the area distribution of the studied city using various LST ranges of different years is shown in Table 4. In 1995, the percentage of land covered by the LST 22–24 °C was the highest (52.7%). While at the same LST interval, it fell to 35.31% and 23.27% for 2009 and 2017, respectively. LST class 24–26 °C increased from 7.1% in 1995, 52.4% in 2009, and 64.6% in 2017. Even though the area with LST of 26–28 °C was higher in 2009

than in 2017, the area with LST > 28 °C was higher in 2017 than in 2009.

The average temperature in the city has continuously risen over the past 22 years, sending a message to residents, policymakers, and environmental experts to take mitigation measures to reverse the situation. Therefore, measuring the changing magnitude of the Dar es Salaam Metropolitan City area's mean LST over time can help understand how the LST pattern changes and make necessary decision-making and associated actions.

Table 4: Land Surface Temperature (LST) percentages for different years

Year	LST (°C)	< 18	18–20	20–22	22–24	24–26	26–28	28–30	>30
1995	Km ²	0.01	8.17	608.38	818.54	110.95	7.25		
	%	0	0.53	39.17	52.7	7.14	0.47		
2009	Km ²	0.08	0.56	33.26	548.49	814.12	228.92	3.65	0.02
	%	0.01	0.04	2.14	35.31	52.41	14.74	0.23	0
2017	Km ²	0.01	0.03	1.63	363.08	1,003.34	203.81	14.63	0.08
	%	0	0	0.1	23.37	64.59	13.12	0.94	0

Relationships between LULC patterns and LST

The relationships between land use land cover (LULC) patterns and land surface temperature (LST) have been expressed in terms of graphical comparison (chord diagrams and cross-section profile) and simple linear regression models.

Graphical comparison using chord diagrams

Figure 4 shows analyses of LST changes by LULC class from 1995 to 2017. The chord diagrams show vegetation, built-up area, water, and bare soil in coverage order. The chord diagrams show that vegetation, water body, and bare-soil areas decreased from 1995 to 2017 while built-up areas increased. The water body has the lowest LST, while built-up has the highest. In 2017, the area under 20–22 °C LST decreased, and high LST increased compared to prior years. LST for water bodies rose from 20 °C in 2009 to 22–24 °C in 2017, and for vegetation, from 20–24 °C to > 24 °C. This pattern suggests that LULC affects LST. More extensive vegetation and water regions lower LST, while built-up areas raise it. Hence, vegetation and bare soil correlate negatively with LST, while built-up cover correlates positively with LST. The findings correspond with those of Saha et al. (2020) in Asia. Open waste incineration, a prevalent practice in DMC, may cause extremely high temperatures in the land covered by vegetation (United Republic of Tanzania 2018). Other factors include forest fires and charcoal (Mligo 2020).

Graphical comparison (cross-sections profiles)

The vertical and horizontal cross-sections have been generated to show the relationships

between the study area's LULC and LST raster data for 1995, 2009, and 2017. The A–B segment represents the horizontal cross-section, while the C–D segment represents the vertical cross-section. The profiling tool extracted the LST pixel values beneath the sections, as shown in Figure 5. The LST is highest in places with more built-up areas and lowest in vegetated areas (Figure 5a), backing up the previous findings on the influence of LULC on LST in Dar es Salaam (Simon et al. 2022). Similarly, the LST values from the horizontal section (A–B) reveal that the LST has risen over time (Figure 5b). The LST is highest in places with more densely built-up areas and lowest at the western and northern points, where the places are rich in woody vegetation, mainly the woodlands and bushlands. The land area with vegetation and bare soil was higher in the early years than in recent years. As a result, LST over the area in the early years was substantially lower than in recent years. However, as these LULC classes were replaced by built-up areas such as buildings, roads, and other impervious surfaces, the LST of these places began to rise drastically. As a result, the 2017 LST profile outperforms previous years' profiles (both in vertical and horizontal sections). The expansion of impervious areas has increased the land surface temperature (LST) in the study area, despite unchanged land use land cover (LULC) in some pixels. This rise in LST is primarily attributed to the increased percentage of impervious surfaces, leading to elevated LST levels in the surrounding areas and highlighting the significant microclimatic effects of LULC changes on temperature patterns (Mensah et al. 2020).

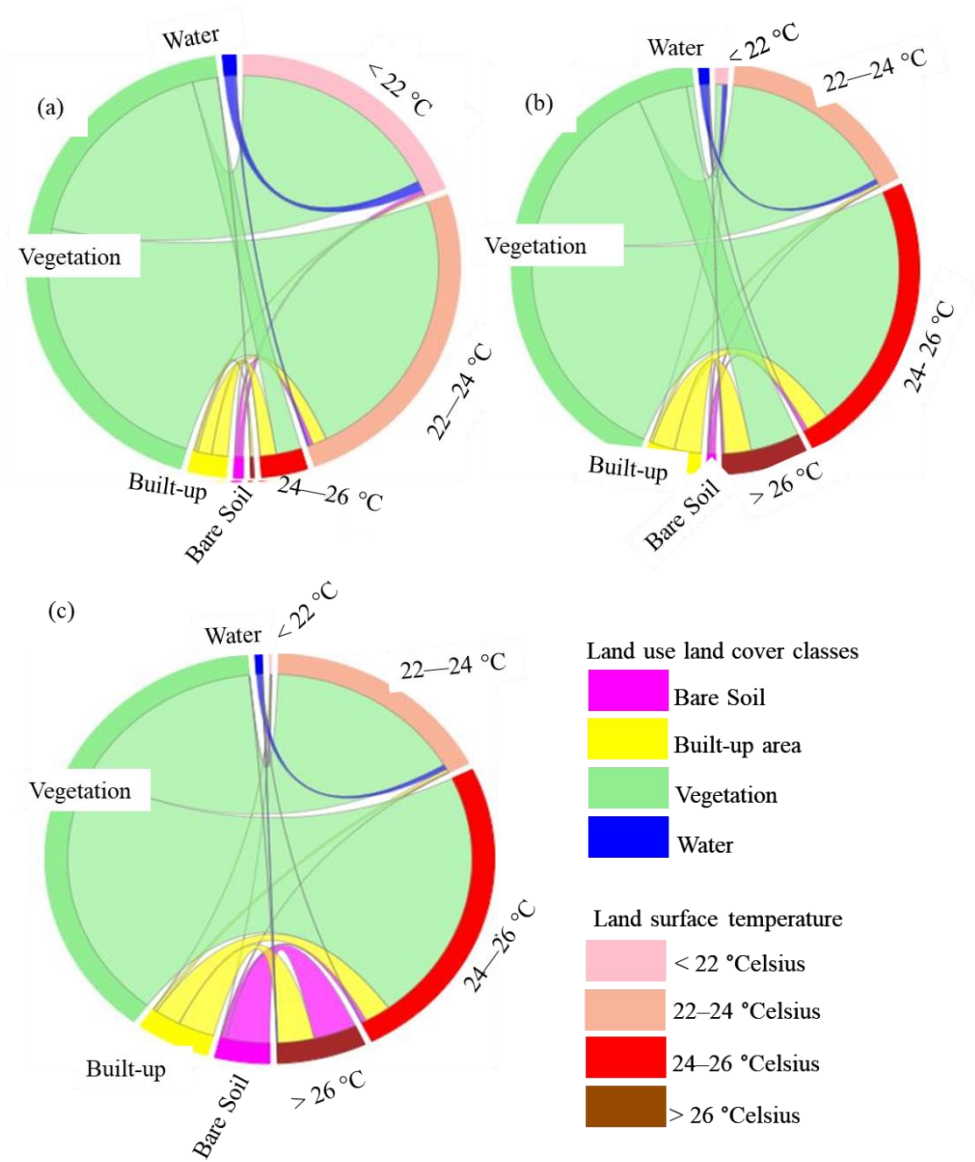


Figure 4: Chord diagrams showing LULC class-wise with LST in Dar es Salaam Metropolitan City (a) year 1995, (b) year 2009, and (c) year 2017.

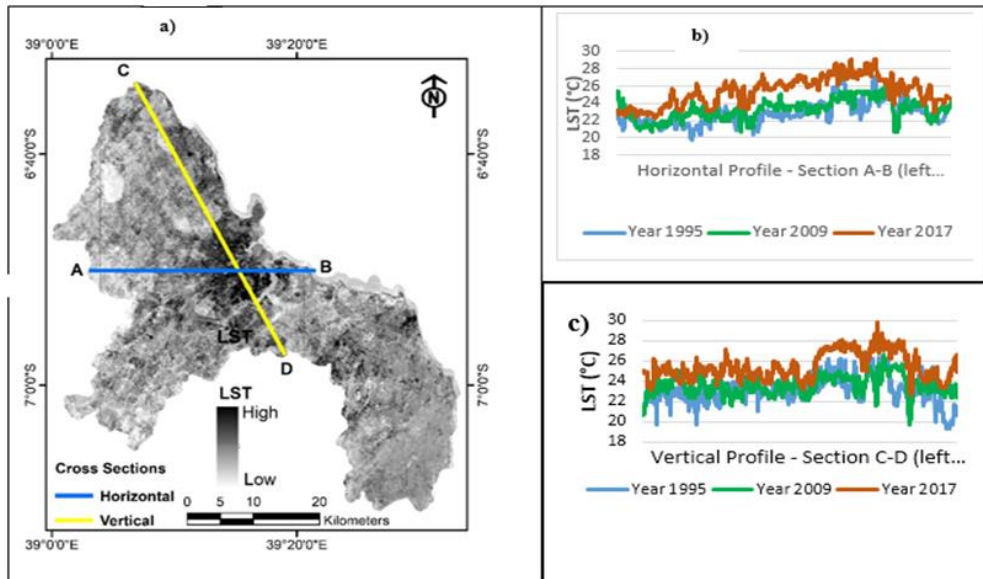


Figure 5: LST and LST cross-section profiles of Dar es Salaam Metropolitan City over different years.

Simple linear regression models

This section describes the relationships between LULC and LST using linear regression models. Because there was only one independent variable and one dependent variable in this study, a Simple Linear Regression Model (SLRM) was used. Each model has an independent variable called LULC and a dependent variable called LST. The model's equations are presented below.

$$LST = -12.776X_{bsl} + 28.08 \tag{9}$$

In equation (9), the independent variable "bare soil" is represented by X_{bsl} . The equation's coefficient is 12.77, and its negative sign indicates a negative correlation between bare soil and the recorded LST. The equation's constant value is 28.08. The model's correlation coefficient (R) value is 0.992, which indicates a strong relationship between bare soil and LST. The coefficient of determination (R^2) value demonstrates that the model can predict 99% of the observed variations. The model's standard error is 0.034 (Table 5). This R-value is the highest among other LULC types, indicating a strong negative correlation with LST. Also, this number indicates that the LST relates to bare soil more strongly than any other LULC in the area.

The independent variable "built-up area" is represented by X_{built} in the equation (10). The equation's coefficient is 7.899, and its sign is positive. The positive sign indicates that the built-up area and LST have a positive association, meaning that as the built-up area increases, the LST also increase.

$$LST = 10.866X_{built} + 21.22 \tag{10}$$

The equation's constant value is 21.22. This model's R-value is 0.795, demonstrating a close correlation between built-up area and LST. Because the R^2 score is 0.632 and the standard error is 0.117, the model can predict around 63% of the variations in the data (Table 5).

The model of vegetation (independent variable) and LST (dependent variable) in equation (11), where X_{veg} denotes the independent variable "vegetation". The equation's coefficient is 88.18, and its sign is negative. The negative sign indicates that the amount of vegetation and LST correlate negatively. The negative correlation means that the LST decreases as vegetation grows. The equation's constant value is 52.424. This model's R-value is 0.774, indicating a strong correlation between vegetation and LST. The R^2 value indicates the model can predict

around 67% of the data variations. In this model, the standard error is 0.014.

$$LST = -88.18X_{veg} + 52.424 \quad (11)$$

In equation (12), the independent variable "waterbody" is represented by X_{water} . The equation coefficient is 112.57, which has a negative sign implying a negative association between the water body area and LST. The constant value in the equation is 58.879. The R (correlation coefficient) value is 0.8252, showing a relatively significant association between the water body and LST. The model's coefficient of determination (R^2) value implies that it can predict a data variability of 82%. The standard error of the model is 0.009 (See Table 5).

$$LST = -112.57X_{water} + 58.879 \quad (12)$$

The analysis of the relationship between LULC change and LST reveals a gradual rise in LST as the built-up area increases, indicating a positive correlation. The correlation coefficient for the built-up area is

0.795, which signifies a significant correlation with LST. Therefore, as the built-up area increases, so does the LST. In contrast, water bodies, vegetation, and bare soil negatively correlate with LST. The correlation coefficients for water bodies, bare soil, and vegetation are -0.908, -0.992, and -0.819, respectively, implying that as the areas covered by water bodies, vegetation, and bare soil decrease, the LST increases, which also conforms with the earlier results and the results of Kabanda (2019) and Naim and Kafy (2021), but differs slightly in the bare soil relationship with LST with previous studies done by Simon et al. (2022).

In conclusion, the regression models are viable because the models' confidence levels were significant ($p < 0.05$). Furthermore, the models' standard errors are tolerable, indicating that the data points are closer to the regression lines, attributing the models as significant.

Table 5: Model summary for the SLRM of LULC and LST

LULU	R	R^2	Adjusted R^2	Std. Error	p-value
Bare soil	-0.992	0.987	0.967	0.034	< 0.05
Water body	-0.908	0.825	0.650	0.009	< 0.05
Vegetation	-0.819	0.671	0.341	0.010	< 0.05
Built-up area	0.795	0.632	0.263	0.117	< 0.05

Conclusion and recommendations

This study used Landsat remote sensing data to investigate changes in land use land cover (LULC) and land surface temperature (LST) in Dar es Salaam Metropolitan City over 27 years. The results revealed that LULC changes in Dar es Salaam affect the city's land surface temperature. The study found that although vegetation presently covers most of the land in the study area (84%), there has been a significant increase in built-up areas at the cost of bare soil and vegetation. Specifically, built-up areas have increased by 8%, whereas vegetation has decreased by 7%, and bare soil has declined by 3%. LST correlates positively with correlation coefficient (R) = 0.795 with the built-up area and negatively with $R = -0.819$, -0.908, and -0.992 with vegetation, water bodies, and bare soil, respectively. Water bodies exhibit the lowest, whereas built-up

areas have the highest LST values. In 2017, the area under 20–22 °C LST decreased, and high LST increased compared to prior years. LST for water bodies rose from 20 °C in 2009 to 22–24 °C in 2017, and for vegetation, from 20–24 °C to > 24 °C, implying that vegetation, bare soil, and water bodies help reduce LST.

Therefore, land use cover changes are crucial in modern resource management and environmental monitoring systems. Thus, land managers and environmentalists should maintain vegetation greenness to reduce LST. In addition, urban green belts and green roofs could mitigate the effects of LST on cities and their surroundings, producing a more inclusive and resilient city. As a result of this research, future studies should focus on how urban residents adapt to rising LST and monitor current LST.

To enhance the comprehensiveness of future studies on land use land cover changes, it is crucial to consider several key factors, including population growth, rates of urbanisation, economic development, policy interventions, agricultural practices, climate change, land ownership patterns, infrastructure development, and the availability and utilisation of natural resources. Additionally, exploring the potential impacts of climatic conditions, demographic trends, and socioeconomic factors on land surface temperature (LST) values is advisable.

Acknowledgements

The authors would like to thank the National Aeronautics and Space Administration (NASA), the United States Geological Survey (USGS) for providing Landsat imagery and the National Bureau of Statistics for providing the administrative boundary of the study area.

Conflicts of Interest

The authors declare that they have no known competing financial interests or personal relationships that could have influenced the work reported in this paper.

References

- Akinyemi FO, Ikanyeng M and Muro J 2019 Land cover change effects on land surface temperature trends in an African urbanising dryland region. *City Environ. Interact.* 4: 1–17.
- Bello-Schünemann J and Aucoin C 2016 *African urban futures*. Australia, Canada, Denmark, Finland, Japan, the Netherlands, Norway, Sweden and the USA.
- Demographia 2022 *Demographia world urban areas—built-up urban areas or world agglomerations*. <http://www.demographia.com/db-worldua.pdf>
- Gohain KJ, Mohammad P and Goswami A 2020 Assessing the impact of land use land cover changes on land surface temperature over Pune city, India. *Quat. Int.* 575: 259–269.
- Guha S, Govil H, Dey A and Gill N 2018 Analytical study of land surface temperature with NDVI and NDBI using Landsat 8 OLI and TIRS data in Florence and Naples city, Italy. *Eur. J. Remote Sens.* 51 (1): 667–678.
- Guha S, Govil H, Gill N and Dey A 2020 Analytical study on the relationship between land surface temperature and land use/land cover indices. *Ann. GIS* 26(2): 201–216.
- Ibrahim I, Abu Samah A, Fauzi R and Noor NM 2016 The land surface temperature impact to land cover types. In: *ISPRS - International Archives of the Photogrammetry, Remote Sensing and Spatial Information Sciences*. pp. 871–876.
- Iqbal MA 2021 Application of regression techniques with their advantages and disadvantages. *Elektron Mag.* 4: 11–17.
- Jaber SM 2019 On the relationship between normalised difference vegetation index and land surface temperature: MODIS-based analysis in a semi-arid to arid environment. *Geocarto Int.* 36 (10): 1–18.
- Kabanda T 2019 Urban heat island analysis in Dar es Salaam, Tanzania. *South Afr. J. Geomat.* 8(1): 98–107.
- Kibassa D and Shemdoo R 2016 Land cover change in urban morphological types of Dar es Salaam and its implication for green structures and ecosystem services. *Mod. Environ. Sci. Eng.* 2 (3): 171–186.
- Manyama MT, Nahonyo CL and Hepelwa AS 2020 Analysis of the Impact of Built Environment on Coastline Ecosystem Services and Values. *East African J. Environ. Nat. Resour.* 2 (2): 44–63.
- Mensah C, Atayi J, Kobo-Bah AT, Švik M, Acheampong D, Kyere-Boateng R, Prempeh NA and Marek M V. 2020 Impact of urban land cover change on the garden city status and land surface temperature of Kumasi. *Cogent Environ. Sci.* 6 (1): 1–16.
- Mligo C 2020 Analyses of Land Cover Changes from 1981 to 2016 in Pande Game Reserve, Tanzania. *Tanz. J. Sci.* 2 (46): 303–316.
- Mnyali ET and Materu SF 2021 Analysis of

- the current and future land use/land cover changes in peri-urban areas of Dar es Salaam City, Tanzania using remote sensing and GIS techniques. *Tanz. J. Sci.* 47 (5): 1622–1636.
- Mzava P, Nobert J and Valimba P 2019 Land cover change detection in the urban catchments of Dar es Salaam, Tanzania using remote sensing and GIS techniques. *Tanzania J. Sci.* 45 (3): 315–329.
- Naim MNH and Kafy A- Al 2021 Assessment of urban thermal field variance index and defining the relationship between land cover and surface temperature in Chattogram city: A remote sensing and statistical approach. *Environ. Challenges* 4: 1–14.
- Noi Phan T, Kuch V and Lehnert LW 2020 Land cover classification using google earth engine and random forest classifier-the role of image composition. *Remote Sens.* 12 (15)
- Saha P, Bandopadhyay S, Kumar C and Mitra C 2020 Multi-approach synergic investigation between land surface temperature and land-use land-cover. *J. Earth Syst. Sci.* 129: 1–21.
- Sekertekin A and Bonafoni S 2020 Sensitivity analysis and validation of daytime and nighttime land surface temperature retrievals from landsat 8 using different algorithms and emissivity models. *Remote Sens.* 12 (17)
- Serra J, Marques R, Augusto C and Santos G 2018 Spatiotemporal impact of land use/land cover changes on urban heat islands: A case study of Paço do Lumiar, Brazil. *Build. Environ.* 136: 279–292.
- Simon O, Yamungu N and Lyimo J 2022 Simulating land surface temperature using biophysical variables related to building density and height in Dar es Salaam, Tanzania. *Geocarto Int.*: 1–18.
- Simwanda M, Ranagalage M, Estoque RC and Murayama Y 2019 Spatial analysis of surface urban heat Islands in four rapidly growing african cities. *Remote Sens.* 11: 1–20.
- Sussman HS, Raghavendra A and Zhou L 2019 Impacts of increased urbanisation on surface temperature, vegetation, and aerosols over Bengaluru, India. *Remote Sens. Appl. Soc. Environ.* 16: 1–12.
- Tewabe D and Fentahun T 2020 Assessing land use and land cover change detection using remote sensing in the Lake Tana Basin, Northwest Ethiopia. *Cogent Environ. Sci.* 6 (1): 1–21.
- United Nations Department of Economic and Social Affairs and Population Division 2019a *World Population Prospects 2019: Highlights.*
- United Nations, Department of Economic and Social Affairs, Population Division 2019b *World urbanisation prospects 2018: highlights (ST/ESA/SER. A/421).*
- United Republic of Tanzania 2022 *2022 Population and Housing Census - Preliminary Report in Swahili Language.* <https://www.nbs.go.tz/index.php>, Tanzania, National Bureau of Statistics.
- United Republic of Tanzania 2018 *Inventory of the waste open burning in Arusha, Tanga and Dar es Salaam cities.* https://stopopenburning.unitar.org/site/assets/files/1093/tanzania_inventory_report-1_for_arusha_tana_and_dar-_received_april2019.pdf
- Xiao H, Kopecká M, Guo S, Guan Y, Cai D, Zhang C, Zhang X and Yao W 2018 Responses of urban land surface temperature on land cover: A comparative study of Vienna and Madrid. *Sustain.* 10 (2): 1–19.
- Young NE, Anderson RS, Chignell SM, Vorster AG, Lawrence R and Evangelista PH 2017 A survival guide to Landsat preprocessing. *Ecology* 98 (4): 920–932.
- Zhang Y and Sun L 2019 Spatial-temporal impacts of urban land use land cover on land surface temperature: Case studies of two Canadian urban areas. *Int. J. Appl. Earth Obs. Geoinf.* 75: 171–181.